Jiang, Y. and Chen, Q. 2002. "Effect of fluctuating wind direction on cross natural ventilation in building from large eddy simulation," *Building and Environment*, 37(4), 379-386.

Effect of fluctuating wind direction on cross natural ventilation in buildings from large eddy simulation

Yi Jiang and Qingyan Chen*
Building Technology Program
Massachusetts Institute of Technology
77 Massachusetts Avenue, Cambridge, MA 02139

Abstract

A large eddy simulation (LES) program with the Smagorinsky subgrid-scale model has been used to study cross natural ventilation in buildings, which has experimental data available from on-site measurements and a wind tunnel. Since natural wind changes direction over time, it is hard to reproduce this effect in a conventional wind tunnel where the "wind" direction is fixed. There are discrepancies between the on-site and wind tunnel cases for the wind-pressure difference across the buildings, the eddy size behind the buildings, and the wind speed distribution inside an apartment with cross ventilation. LES can successfully simulate both cases by changing or fixing incoming wind direction, and the simulated results agree reasonably with the corresponding experimental data.

Keywords: Cross natural ventilation; Large eddy simulation

1. Introduction

Natural ventilation, a passive-cooling method for buildings, can improve indoor air quality [1], provide a high level of thermal comfort [2], and reduce energy consumption in buildings [3]. As a result, the study of natural ventilation has gained more and more attention in recent years.

Cross ventilation is a major type of natural ventilation. In order to successfully design cross ventilation, it is necessary to obtain detailed information of air and pressure distributions in and around buildings. Although full-scale measurements for a building site can provide reliable data, the experiment is time consuming and hard to control. In addition, the data are limited and not very informative. In most cases, the experimental data obtained from one building site may not be extended to another because of different weather data and building surroundings. Another approach is the use of small-scale models in a wind tunnel to simulate natural ventilation. In general, the mean flow characteristics, such as mean pressure, can be adequately modeled for a single building [4, 5]. However, the fluctuating components of the flow characteristics are difficult to reproduce [6, 7]. Therefore, the data obtained from a wind tunnel measurement may lead to a significant error. An alternative approach to study the airflow in and around buildings is computational fluid dynamics (CFD). CFD is becoming popular due to its informative results and low labor and equipment costs, as a result of the development in turbulence modeling and computer speed and capacity.

Three different CFD methods are available: direct numerical simulation (DNS), large eddy simulation (LES), and Reynolds averaged Navier-Stokes (RANS) modeling. DNS cannot be used to study natural ventilation due to the limitations of available computer memory and speed at present. LES separates flow motions into large eddies and small eddies. LES computes the

* Corresponding author. Tel.: 1-617-253-7714; Fax: 1-617-253-6152; Email: qchen@mit.edu

large eddies in a three-dimensional and time dependent way while modeling the small eddies with a subgrid-scale model. In recent years, LES has been successfully applied to several airflows related to buildings [8-10]. RANS modeling determines time-averaged flow parameters, such as mean air velocity and temperature, by using a turbulence model. RANS modeling requires less computing time than LES because it solves mean flow parameters. Therefore, RANS modeling is the most widely used CFD method in many industrial applications. To simulate natural ventilation in buildings, however, RANS modeling has some deficiencies.

First, RANS modeling cannot correctly predict airflow around buildings. Lakehal and Rodi [11] compared the computed results of airflow around a bluff body by using various RANS and LES models. They found that most RANS models had difficulties generating the separation region on the roof, which was observed in the experiment. Furthermore, all of the RANS models over-predicted the recirculation region behind the body. On the other hand, the LES models did not encounter these problems, and their results agreed well with the experimental data. Secondly, natural wind varies in both speed and direction, which needs a transient simulation. With RANS modeling, a quasi-steady solution can be obtained at each time step. However, whether this quasi-steady results can represent a real transient condition is still in doubt, and the computing time may not be much less than that required by LES.

Hence, the present investigation will study cross ventilation in buildings by using LES with the Smagorinsky subgrid-scale model. Katayama et al. [12] measured detailed flow information for this case, which will be used to validate the numerical results obtained in this investigation.

2. Large eddy simulation

This section will briefly discuss the governing equations of LES, the subgrid-scale model used, and the numerical scheme employed for solving the equations.

2.1 Governing equations

By filtering the Navier-Stokes and continuity equations, one would obtain the governing equations for the large-eddy motions as

$$\frac{\partial \overline{u_i}}{\partial t} + \frac{\partial}{\partial x_j}(\overline{u_i} \cdot \overline{u_j}) = -\frac{1}{\rho}\frac{\partial \overline{p}}{\partial x_i} + \nu \frac{\partial^2 \overline{u}_i}{\partial x_i \partial x_j} - \frac{\partial \tau_{ij}}{\partial x_j} \qquad (1)$$

$$\frac{\partial \overline{u_i}}{\partial x_i} = 0 \qquad (2)$$

where u_i = component of the velocity vector in the x_i direction
u_j = component of the velocity vector in the x_j direction
ρ = air density
p = air pressure
τ_{ij} = subgrid scale Reynolds stresses
ν = kinetic viscosity

The bar represents grid filtering. For example, a one-dimensional filtered velocity can be obtained from

$$\overline{u_i} = \int G(x, x') u_i(x) dx' \tag{3}$$

where $G(x, x')$, the filter kernel, is a localized function. $G(x, x')$ is large only when (x-x′) is less than a length scale or a filter width. The length scale is a length over which averaging is performed. Flow eddies larger than the length scale are "large eddies" and smaller than the length scale are "small eddies". The current study uses a box filter:

$$G(x_i) = \begin{cases} \dfrac{1}{\Delta_i} & (|x_i| \le \dfrac{\Delta_i}{2}) \\ 0 & (|x_i| > \dfrac{\Delta_i}{2}) \end{cases} \tag{4}$$

where Δ_i is the filter width.

In the above LES governing equations, the subgrid-scale Reynolds stresses in Eq. (1),

$$\tau_{ij} = \overline{u_i u_j} - \overline{u}_i \cdot \overline{u}_j \tag{5}$$

are unknown and must be modeled. The following section discusses the modeling techniques.

2.2 Subgrid model

The present study uses the Smagorinsky subgrid-scale model [13] to model the subgrid-scale Reynolds stresses. The model is the first subgrid-scale model of LES, and has been widely used since the pioneer work by Deardorff [14]. The Smagorinsky model assumes that the subgrid-scale Reynolds stresses, τ_{ij}, are proportional to the strain rate of the tensor, $\overline{S}_{ij} = \frac{1}{2}(\frac{\partial \overline{u}_i}{\partial x_j} + \frac{\partial \overline{u}_j}{\partial x_i})$,

$$\tau_{ij} = -2\upsilon_{SGS}\overline{S_{ij}} \tag{6}$$

where υ_{SGS} is the subgrid-scale eddy viscosity defined as

$$\upsilon_{SGS} = (C_{SGS}\Delta)^2 |\overline{S}| = (C_{SGS}\Delta)^2 (2\overline{S_{ij}} \cdot \overline{S_{ij}})^{\frac{1}{2}} \tag{7}$$

where C_{SGS} = 0.1 ~ 0.2 is the Smagorinsky constant, which varies according to flow types. The Smagorinsky model is an adaptation of the mixing length model of RANS modeling to the subgrid-scale model of LES.

The Smagorinsky model has been widely applied to airflows around buildings [15], in building [9, 10], and cross ventilation in a wind tunnel [16]. The results are generally within good agreement of the experimental data.

2.3 Numerical scheme

With the subgrid-scale model, the present study uses the simplified marker and cell method (SMAC) [17] to solve the governing equations of LES. In order to correlate the momentum equation and the continuity equation, SMAC method first solves the momentum equations without the pressure term. So the obtained velocity, $\overline{u}_i^*$, is a pseudo-velocity.

$$\frac{\partial \overline{u}_i^*}{\partial t} + \frac{\partial}{\partial x_j}(\overline{u}_i \cdot \overline{u}_j) = \nu \frac{\partial^2 \overline{u}_i}{\partial x_i \partial x_j} - \frac{\partial \tau_{ij}}{\partial x_j} \tag{8}$$

Subtracting Eq. (1) from Eq. (8) yields:

$$\frac{\partial(\overline{u}_i^* - \overline{u}_i)}{\partial t} = \frac{1}{\rho}\frac{\partial p}{\partial x_i} \tag{9}$$

Then by placing divergence on both sides of Eq. (9) and using Eq. (2), we have

$$\frac{\partial}{\partial t}\left(\frac{\partial \overline{u}_i^*}{\partial x_i}\right) = \frac{1}{\rho}\frac{\partial^2 p}{\partial x_i^{\,2}} \tag{10}$$

Eq. (10) is a Poisson equation, which can be solved by a strong-implicit procedure [18]. With the solution of the Poisson equation for pressure, the real velocity can be calculated with

$$\overline{u}_i = \overline{u}_i^* - \frac{\Delta t}{\rho}\frac{\partial p}{\partial x_i} \tag{11}$$

The current study uses a finite difference method to discretize the governing equations. Since the discretion of convection terms is a major source of numerical errors in LES calculation, it is very important to choose a proper scheme to discretize the convection terms. Although an upwind scheme to discretize the convection terms can provide a stable result, it introduces a built-in numerical dissipation that can be larger than the dissipation introduced by the subgrid-scale stresses. Mittal and Moin [19] found that the upwind scheme produces poor velocity power spectra compared with the central scheme. Therefore, the current calculation uses second-order central differencing scheme to discretize the convection terms. This central differencing scheme may exhibit oscillating behavior, due to an insufficient grid resolution. Nevertheless, the convection terms should not be solved by the upwind scheme, especially the lower order of upwind scheme [20].

The time term in the filtered Navier Stokes equations is discretized by the explicit Adams-Bashforth scheme, which is also a second-order differencing scheme. Finally, a staggered variable configuration is used to eliminate the need for a pressure boundary condition.

3. On-site and wind tunnel measurements

Katayama et al. [12] performed on-site measurements and wind tunnel tests for both indoor and outdoor airflows in a building site as shown in Fig. 1. This site lies to the south of the Japanese Sea, and is seven kilometers away from the nearest beach. There is an open field located between the beach and the building site. The prevailing wind during the experimental period was from the north and northwest directions.

The incoming wind profile at Location R (Fig. 1) was measured on-site using a balloon system (a 3-cup anemometer) at 15 points ranging from 2 m to 160 m high [21]. The wind-pressure difference across an apartment was measured at Buildings A through D. Those buildings are identical five-story buildings with eight apartments on each floor. Fig. 2 shows the locations of those apartments where the pressure differences were measured, which varied from one building to another one. Fig. 3 diagrams those identical building, and gives the overall dimensions of the buildings: 56.43 m × 13.96 m × 6.66 m. The location marked as "indoor" in Fig. 3 is an apartment in Building A where indoor airflow was measured at a height of 1.2 m from the floor. The wind speed at the center of the north window (Fig. 3) was also recorded as a reference.

Katayama et al. [12] have done two wind tunnel tests of airflow in and around the buildings. The first test included about twenty buildings on the site with a model scale of 1/300, where the wind pressure differences around Buildings A through D were measured. The second test used only Building A with a model scale of 1/20 in order to obtain the detailed distributions of indoor airflow.

4. Results and Discussion

The LES model has been applied to study cross ventilation in buildings. The incoming wind to the building site and the computational domain size are the two key issues for studying airflow in and around buildings correctly and efficiently with LES. The following two sections will discuss how to simulate the incoming wind and how to determine the computational domain to provide correct results with affordable computing time with LES. Then, the computational results will be compared with the experimental data for airflow distributions in and around buildings.

4.1 Wind Simulation

The on-site measurements and wind tunnel experiments provide two sets of data on the incoming wind, both with a 1/4 power law mean-wind profile and the same turbulent intensity. However, Katayama et al. [12] noticed that there exist some discrepancies about the wind-pressure differences across Buildings C and D and the indoor airflow distributions between these two sets of data. They explained that the discrepancies were due to the fluctuations of natural wind. The natural wind was highly variable in both speed and direction, which cannot be easily generated in a wind tunnel. As pointed out by Surry [7], Lin et al. [22], and Zhao [23], the wind direction is fixed in a conventional wind tunnel, which is different from real wind whose direction and speed vary over time. Hence, using a tunnel-generated wind to simulate real wind may cause significant errors.

Although natural wind direction changes over time, its histogram exhibits some rules. Nitta [24] observed that, at a high wind speed (4.46 m/s), the histogram follows a normal distribution. At a low wind speed (1.17 m/s), however, the histogram tends to be uniform. Fig. 4 shows the wind data from on-site measurement of a campus. The results present similar conclusions.

Due to different characteristics of natural wind and the incoming flow from a wind tunnel, LES in this investigation used different approaches to simulate the incoming flow. For the wind tunnel case, LES fixed the wind direction. For the on-site case, LES simulated the wind with either a normal or a uniform distribution depending on the magnitude of the incoming wind speed. Since the on-site measurement did not measure the variation of the incoming wind direction, the present investigation used the variation from other studies. Zhao [23] found that a typical variation of wind direction is about 80^o during a time period of 15 minutes. Because the real time in our simulations was about 10~20 minutes, the variation of wind direction was set to be 80^o. The incoming wind speed ranged from 0.5~4 m/s above the building roof according to the on-site measurements. The wind speed below the roof level would be much lower than this range. Therefore, the present study assumed that the variation of the incoming wind direction was with a uniform distribution.

4.2 Determination of computational domain

The computational domain in LES must be large enough to generate correct flow information around the buildings. However, if the domain is too large, the computing time will be increased significantly. The outdoor measurements were performed only on Buildings A through D, and indoor measurements were conducted inside an apartment in Building A. Hence, our computational effort was to ensure correct simulation of the flow distributions around Buildings A through D and inside the apartment in Building A.

Since the wind was directed from northwest, Buildings A through D were in the upwind direction. If we include ten buildings in LES as shown in Fig. 1, the impact of the side and rear buildings on the flow distributions around Buildings A through D should be correctly simulated. For the study of the indoor airflow in the apartment in Building A, the computational grid size should be at least 0.2 m and the time step size should be sufficiently small (0.05 seconds) in order to obtain a stable simulation and detailed flow information. Even with a non-uniform grid system, the total grid number would be as high as eight million. This would require three months of computing time on a fast workstation. To save computing time, the indoor and outdoor calculations were separated.

The airflow distributions outside of buildings depend on the incoming wind speed and direction, the building size and shape, and the size and location of the building opening. If the size of the building openings is less than 1/6 of the total facade area, the effects of these openings on the outdoor airflow distributions can be neglected [25]. Since, the building opening area on the site was much smaller than 1/6 of the total facade area, the ten buildings can be set as concrete blocks. As a result, the smallest grid can be as large as 1 m and the corresponding time step can be as large as 0.1 seconds without numerical stability problems.

The study of the indoor airflow in Building A needs correct flow information around the building itself. Therefore, the computational domain can be much smaller compared with that for the outdoor airflow study. Since Building A is in the windward direction, a computational domain that includes four buildings (A, B, E and F as shown Fig. 1) would be sufficient. To ensure that this reduction in computational domain size can still generate correct airflow

distribution around building A, the computed results with the small domain (four buildings) were compared with those with the large domain (ten buildings). The pressure difference between these two cases is less than 5% in the most regions of Building A, which is satisfactory for ventilation design. The separation of indoor and outdoor airflow calculations can reduce the computing time dramatically compared with the calculation of both indoor and outdoor flow simultaneously. Table 1 illustrates the computing time with different domains.

4.3 Outdoor airflow distribution

Fig. 5 shows the mean velocity distributions with two different wind conditions. When the wind is fixed from the northwest direction, the recirculation regions behind Buildings A through D are much larger than in the case where the wind direction varies from the north to west with a mean direction of northwest. With a fixed wind direction, the wind blows to only certain regions of a building. There are some regions, such as those behind the building, where the wind can hardly reach. Therefore, large recirculation zones can be easily formed in these regions. On the other hand, with a variable wind direction, the wind will blow from west at some moments (from the bottom to the top in Fig. 5). The west wind would destroy the formation of the large recirculation zones behind the buildings that leads to much smaller eddies. The different airflow distributions would cause different pressure distributions around the buildings.

Table 2 presents the pressure coefficients ($\Delta Cp = \frac{P_{North} - P_{south}}{1/2\rho V_{ref}^2}$) at the selected apartments in Buildings A through D. For Buildings A and B, the measured ΔCp values from the wind tunnel agree well with that from the on-site measurements. LES also gave reasonable results for two different wind conditions. For Buildings C and D, both the wind tunnel measurements and LES, with the fixed wind direction, show similar results. However, the wind tunnel over-predicted ΔCp values by nearly four times compared with the data obtained from on-site measurements. The LES results with varied wind direction are in good agreements with the on-site data. These results show that directional fluctuations of an incoming wind play an important role in determining wind pressure distributions around buildings. Unfortunately, this directional fluctuation is hard to be produced in a wind tunnel.

Fig. 6 shows the distribution of pressure coefficient difference, ΔCp, across Building D (the other buildings show similar patterns). When the wind direction varied from north to west, airflow was able to pass along the east-west facades of the building at times. This flow reduced the eddy size, and evened out the pressure gradient along the building facades.

4.4 Indoor airflow distribution

The indoor airflow study calculated only airflow around four buildings (Buildings A, B, E and F) and in Building A as shown in Fig. 1. Fig. 7 shows the wind speed distribution inside the apartment in Building A. The wind-tunnel data present a deep, thin and high velocity core in the north room (upper room). The LES results with fixed wind direction show a similar flow pattern. The on-site measurements show a shallower and wider high-speed region in both rooms. The LES results with the varied wind direction are in reasonable agreement with the on-site data. Note that LES with Smagorinsky subgrid-scale model may not accurately predict indoor airflow (Zhang and Chen, 2000). A perfect agreement between the LES results and the experimental data is difficult to achieve with the Smagorinsky model.

These results illustrate that, with a fixed wind direction, the wind can pass through the room openings without too much oscillation and energy loss. Hence, a deep, thin and high-speed core is formed. On the other hand, with varied wind directions, the flow dissipates energy to the corners of the room, which reduces the depth and width of the high-speed core. The wind speed becomes evenly distributed throughout the room than that with a fixed wind direction.

5. Conclusions

LES with the Smagorinsky subgrid-scale model has been used to simulate cross natural ventilation in buildings. The experimental data from wind tunnel and on-site experiments from the literature have been used to validate the computed results. The computed airflow results, such as pressure coefficients and air velocity distributions, agree reasonably with the experimental data.

Natural wind changes direction over time, which is hard to produce in a conventional wind tunnel. LES can simulate both cases by adjusting inlet boundary conditions: a fixed incoming wind direction for the wind-tunnel test, and a varied incoming wind direction for the on-site measurements. The measured data and computed results show three significant differences in the airflows for a real building site and for a wind tunnel.

(1) Natural wind at some moments can destroy the formation of large recirculation zones behind a building, and only small eddies can exist. With a fixed wind direction in the wind tunnel, the wind cannot reach some regions of the building façades. Therefore large recirculation zones are easily formed in the downwind direction.

(2) The gradient of the pressure coefficient difference across the building, ΔCp, is more uniform with a varied wind direction than that with a fixed wind direction.

(3) The indoor airflow with a fixed wind direction has a thinner, deeper and higher speed core than that with a variable wind direction. This is because the wind in the former case does not oscillate and loses less energy.

Acknowledgment

This work is supported by the U.S. National Science Foundation under grant CMS-9877118. We would like to thank Professor Tadahisa Katayama from Kyushu University, Japan for providing the experimental data and building plans and for many useful discussions.

References

[1] Finnegan, J.J., Pickering, C.A.C. and Burge, P.S. The sick building syndrome: prevalence studies. British Medical J. 1984; 289: 1573-1575.

[2] Zhao, R., and Xia, Y. Effective non-isothermal and intermittent air movement on human thermal responses. Proc. of Roomvent 98, Stockholm, 1998; 2: 351-357.

[3] Busch, J.F. A tale of two populations: thermal comfort in air-conditioned and naturally ventilated offices in Thailand. Energy and Buildings 1992; 18 (3-4): 235-249.

[4] Dagliesh, W.A. Comparison of model/full-scale wind pressures on high-rise building. J. Ind. Aerodyn. 1975; 1: 55-66.

[5] Petersen, R.L. Wind tunnel investigation of the effect of platform-type structures on dispersion of effluents from short stacks. J. Air Pollution Control Association 1987; 36: 1347-1352.
[6] Tieleman, H.W., Akins, R.E., and Sparks, P.R. A comparison of wind-tunnel and full-scale wind pressure measurements on low-rise structures. J. Wind Eng. Ind. Aerodyn. 1981; 8: 3-19.
[7] Surry, D. Pressure measurements on the Texas Tech Building-II: Wind tunnel measurements and comparison with full scale. Proceedings of the 8th colloquium on Industrial Aerodynamics, Aachen, West Germany, September 4-7, 1989; 25-35.
[8] Murakami, S. Overview of turbulence models applied in CWE-1997. J. Wind Eng. Ind. Aerodyn. 1998; 74-76: 1-24.
[9] Emmerich S.J. and McGrattan, K.B. Application of a large eddy simulation model to study room airflow. ASHRAE Transactions 1998; 104: 1128-1140.
[10] Zhang, W. and Chen, Q. Large eddy simulation of indoor airflow with a filtered dynamic subgrid scale model. International J. Heat and Mass Transfer 2000; 43 (17): 3219-3231.
[11] Lakehal D. and Rodi, W. Calculation of the flow past a surface-mounted cube with two-layer turbulence models. J. Wind Eng. Ind. Aerodyn. 1997; 67/68: 65-78.
[12] Katayama T., Tsutsumi J., and Ishii A. Full-scale measurements and wind tunnel tests on cross-ventilation. J. Wind Eng. Ind. Aerodyn. 1992; 41-44: 2553-2562.
[13] Smagorinsky, J. General circulation experiments with the primitive equations. I. The basic experiment. Monthly Weather Review 1963; 91: 99-164.
[14] Deardorff, J.W. A numerical study of three-dimensional turbulent channel flow at large Reynolds numbers. J. Fluid Mech. 1970; 41: 453-480.
[15] Rodi, W., Ferziger, J.H., Breuer M., and Pourquié, M. Status of large eddy simulation: results of a workshop. J. Fluids Eng. 1997; 119: 248-262.
[16] Kato S, Murakami S., Mochida, A, Akabyashi S., Tominaga Y. Velocity-pressure field of cross ventilation with open windows analyzed by wind-tunnel and numerical-simulation. J. Wind Eng. Ind. Aerodyn. 1992; 44 (1-3): 2575-2586.
[17] Harlow F.H. and Welch, J.E. Numerical calculation of time-dependent viscous incompressible flow. Phys. Fluids 1965; 8 (12): 2182-2189.
[18] Stone, H.L. Iterative solution of implicit approximations of multidimensional partial differential equations. SIAM J. Numerical Analysis 1968; 5 (3): 530-558.
[19] Mittal R. and Moin P. Suitability of upwind-biased finite-difference schemes for large eddy simulation of turbulent flows. AIAA J. 1997; 35 (8): 1415-1417.
[20] Shah, K.B. Large eddy simulations of flow past a cubic obstacle. Ph.D. dissertation, Department of Mechanical Engineering, Stanford University, 1998.
[21] Katayama, T. Tsutsumi, J. Ishii, A. Nishida, M. and Hashida, M. Observations of heat flux in an urban area with a large pond by kytoons. J. Wind Eng. Ind. Aerodyn. 1989; 32: 41-50.
[22] Lin, J.X., Surry, D., and Tieleman, H.W. The distribution of pressure near roof corners of flat roof low buildings. J. Wind Eng. Ind. Aerodyn. 1995; 56: 235-265.
[23] Zhao, Z. Wind flow characteristics and their effects on low-rise buildings. Ph.D. dissertation, Department of civil engineering, Texas Tech University, 1997.
[24] Nitta K. Cross-correlation between speed and direction of urban wind fluctuation. Energy and Buildings 1990/1991; 15-16: 357-363.
[25] Vickery, B.J., and Karakatsanis, C. External pressure distributions and induced internal ventilation flow in low-rise industrial and domestic structures. ASHRAE Transactions 1987; 98(2): 2198-2213.

Figure Captions

Fig. 1 Layout of the building group.
Fig. 2 The locations of the apartments where wind pressure difference across the buildings was measured.
Fig. 3 The overall dimensions of the building (Length × height × width = 56.43 m × 13.96 m × 6.66 m), and the location of an apartment in Building A where indoor airflow was measured at a height of 1.2 m from the floor (north side elevation).
Fig. 4 Comparison of the histograms of wind data.
Fig. 5 The mean velocity distributions around the buildings at 3 m from the ground.
(a) With fixed wind direction from northwest
(b) With a variable wind direction from north to west and a mean direction from northwest
Fig. 6 The ΔCp distributions across Building D.
(a) With fixed wind direction from northwest
(b) With a variable wind direction from north to west and a mean direction from northwest
Fig. 7 Comparisons between the experimental data and LES results.
(a) Wind-tunnel
(b) LES (fixed direction)
(c) On-site
(d) LES (varied direction)

Tables

Table 1
Comparison of total CPU time among different domain size and cell size

No. of bldgs	Include indoor?	Domain size L×W×H (m×m×m)	Smallest grid size	Total grid number	Time step (s)	Total real time (min)	Total CPU (days)
10	Yes	$450 \times 80 \times 400$	0.2 m*	8×10^6	0.05	20	88
10	No	$450 \times 80 \times 400$	1.0 m	0.5×10^6	0.1	20	2.8
4	Yes	$250 \times 60 \times 280$	0.2 m*	1.8×10^6	0.05	10**	6

* Smaller cell size due to indoor calculation needs smaller time step size in order to stabilize the computation.
** A smaller domain requires a smaller total real time used in the simulation because the time for the wind to travel from one end to another is faster.

Table 2
ΔCp at selected apartments in Buildings A through D

	Building A	Building B	Building C	Building D
On-site measurements	0.85	0.42	0.12	1.03
LES (varied wind direction)	0.87	0.43	0.20	1.00
Wind tunnel measurements	0.85	0.42	0.46	1.26
LES (fixed wind direction)	0.90	0.45	0.50	1.25

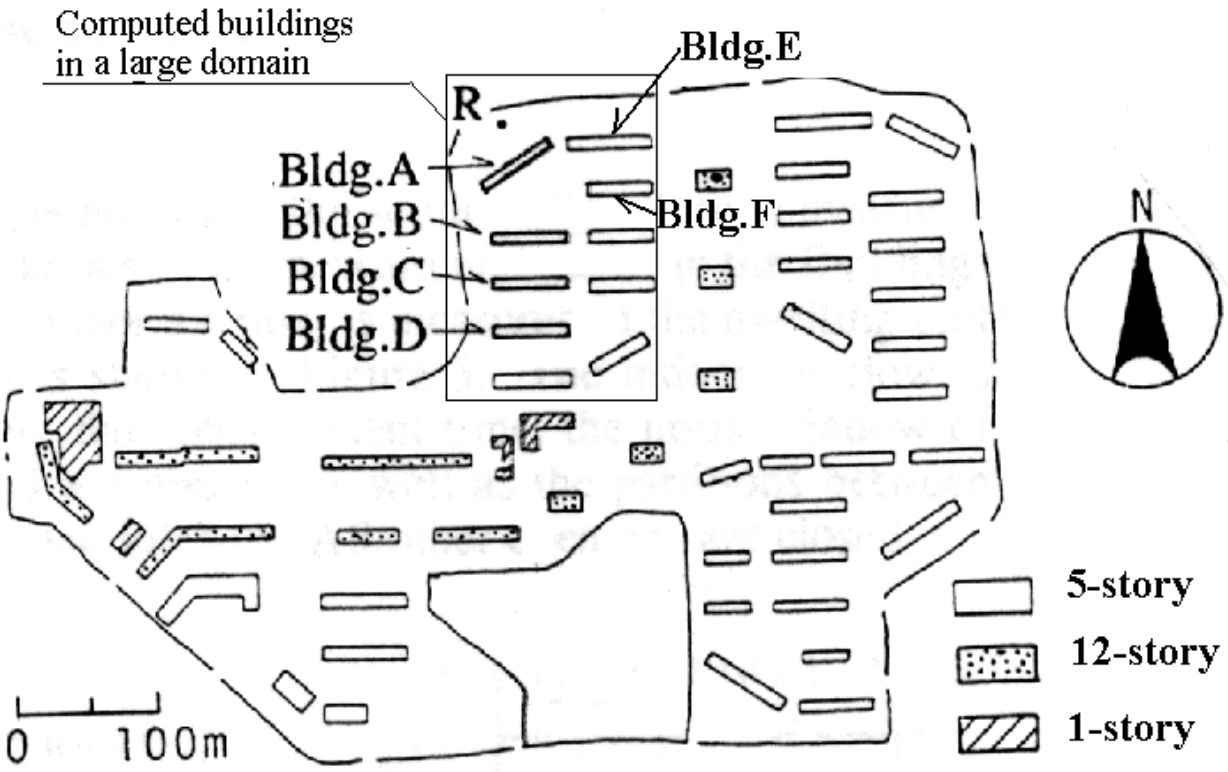

Fig. 1 Layout of the building group

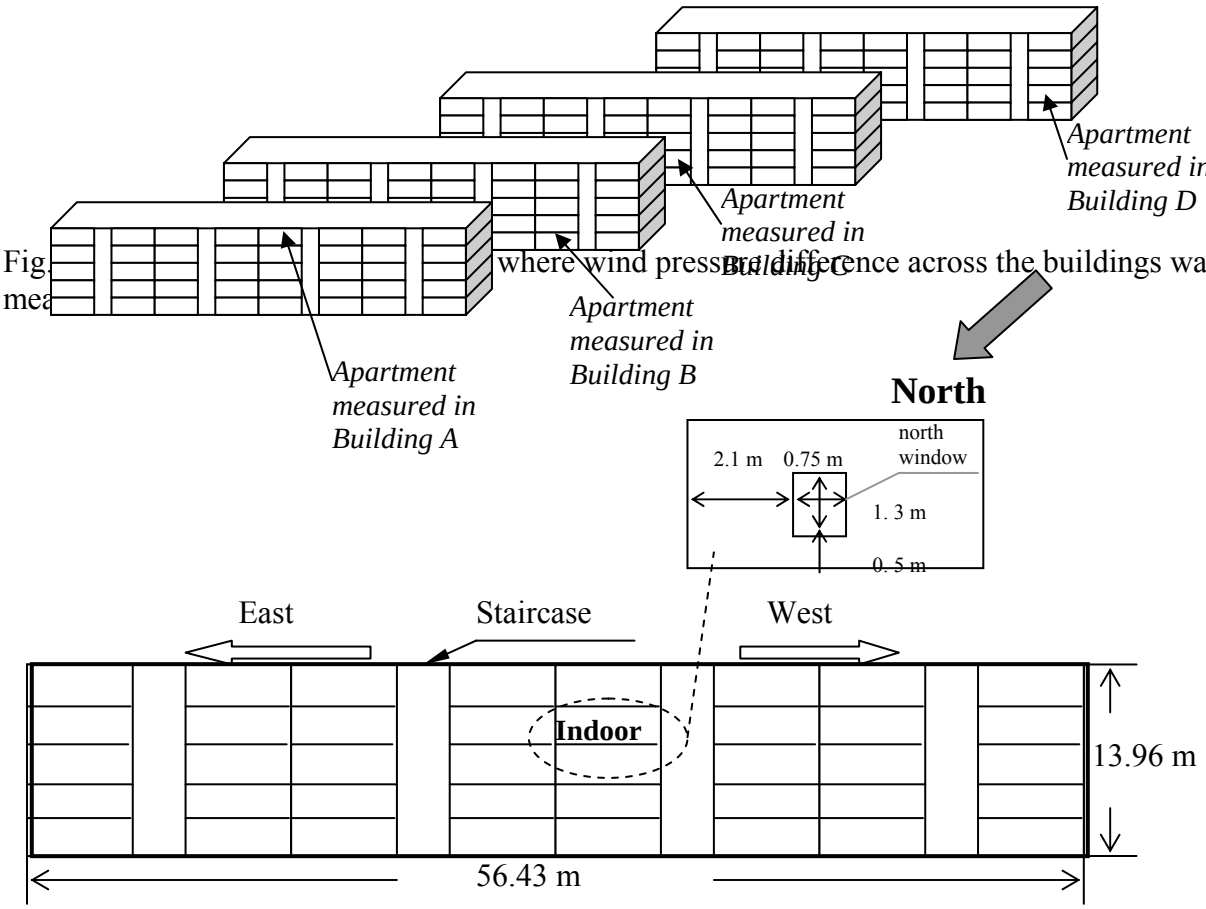

Fig. 3 The overall dimensions of the building (Length × height × width = 56.43 m × 13.96 m × 6.66 m), and the location of an apartment in Building A where indoor airflow was measured at a height of 1.2 m from the floor (north side elevation).

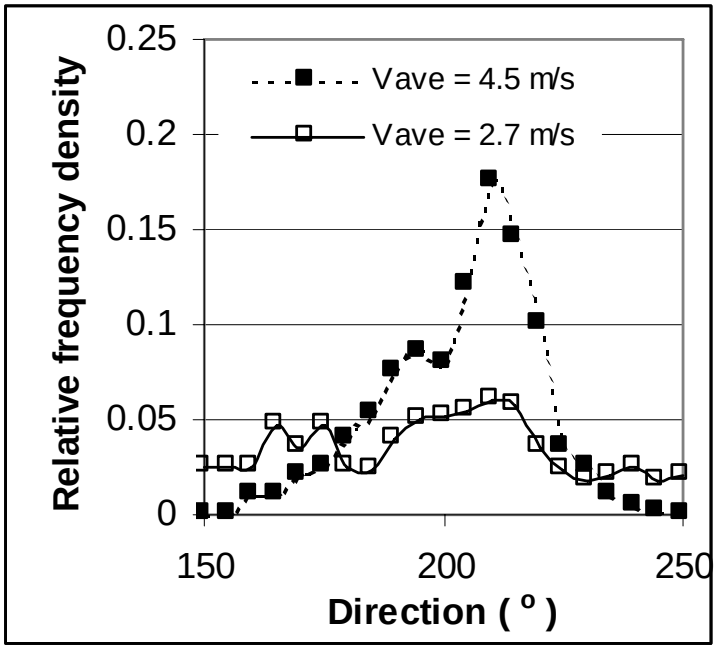

Fig. 4 Comparison of the histograms of wind data.

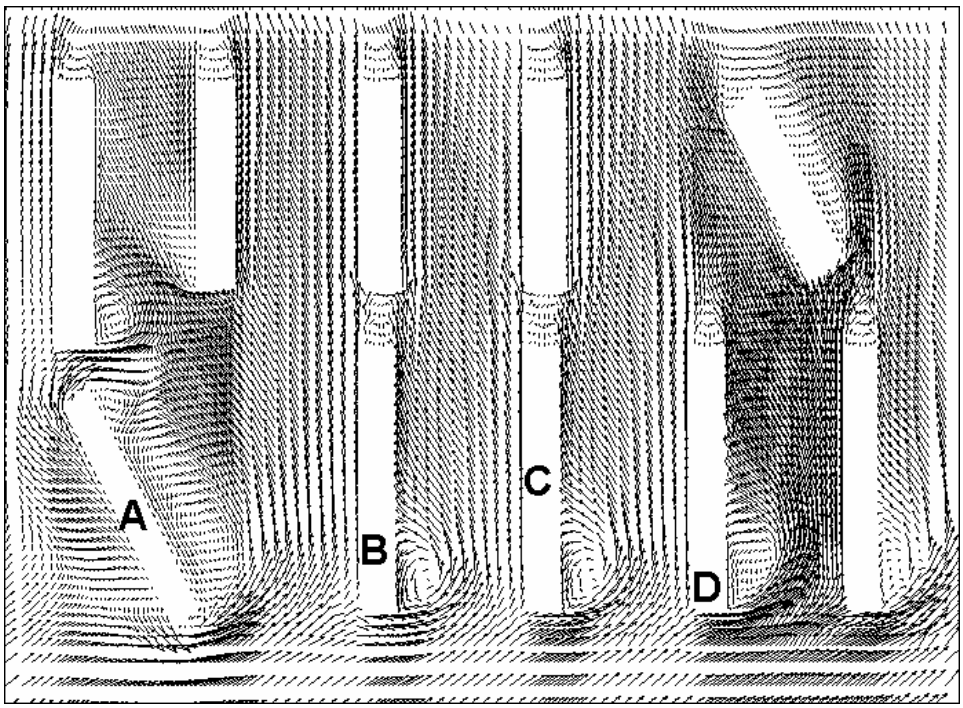

(a)

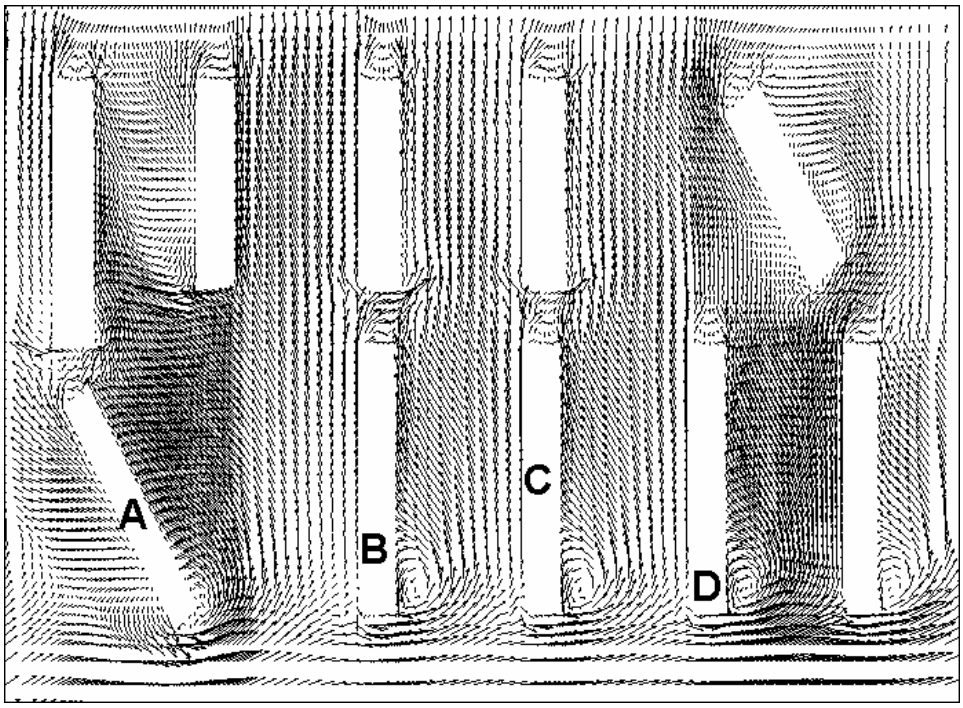

(b)

Fig. 5 The mean velocity distributions around the buildings at 3 m from the ground (a) With fixed wind direction from northwest; (b) With a variable wind direction from north to west and a mean direction from northwest.

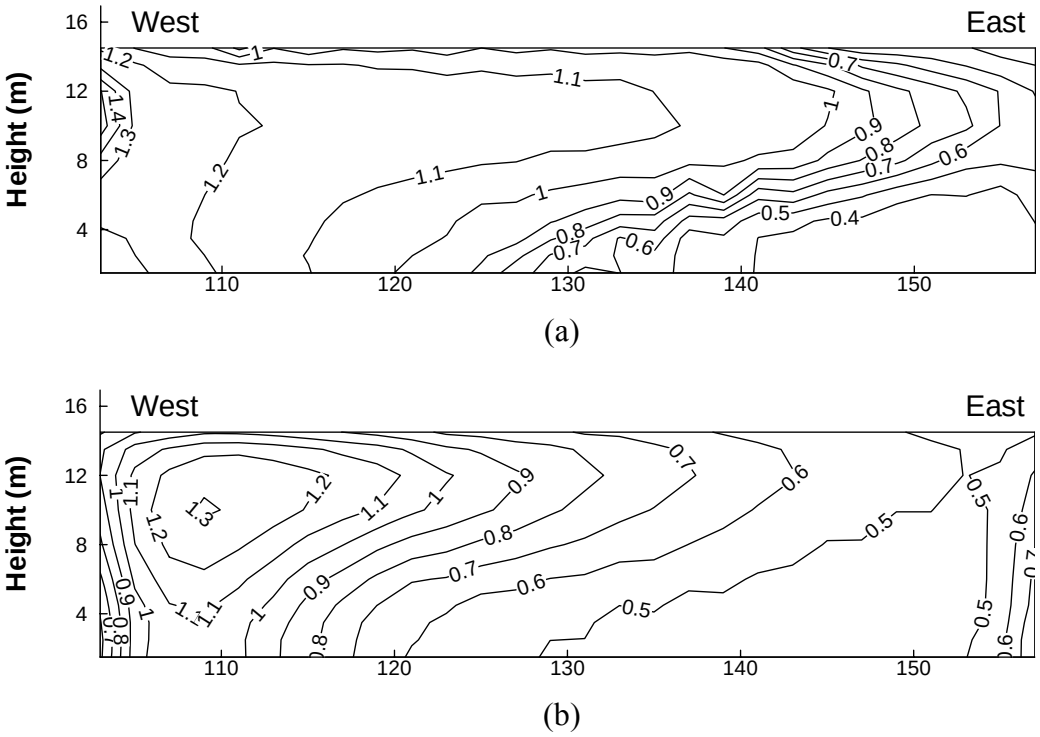

Fig. 6 The ΔCp distributions across Building D (a) With fixed wind direction from northwest; (b) With a variable wind direction from north to west and a mean direction from northwest

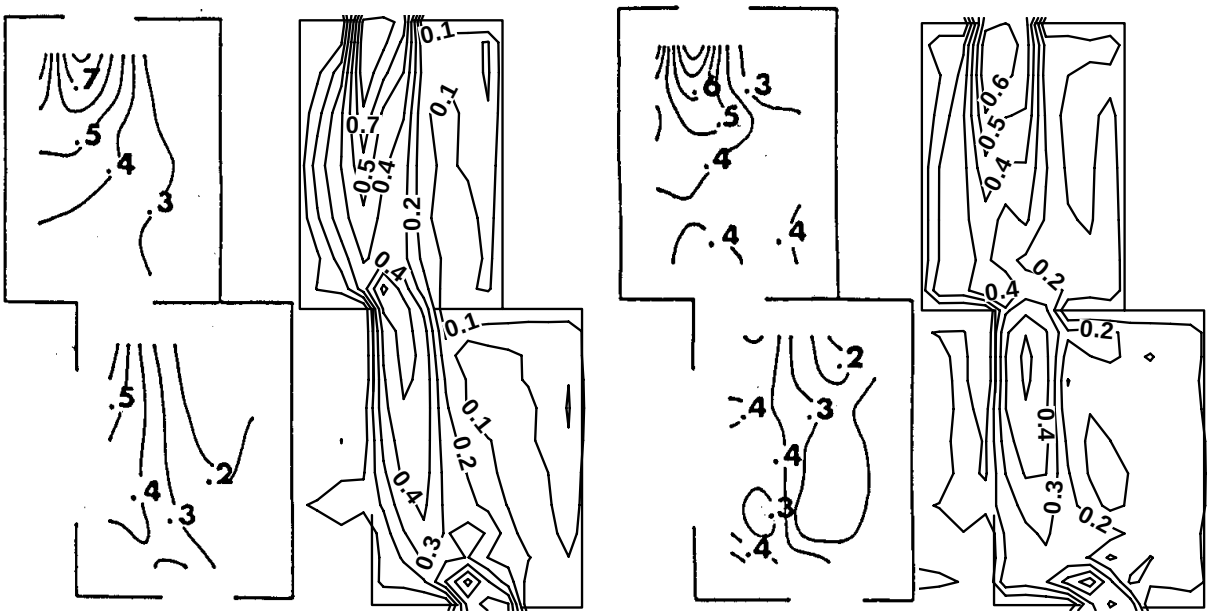

Fig. 7 Comparisons between the experimental data and LES results. (a) Wind-tunnel; (b) LES (fixed direction); (c) On-site; (d) LES (varied direction).